

ORIGINAL ARTICLE - GASTROENTEROLOGY (EXPERIMENTAL)

Effects of fecal stream deprivation on human intestinal barrier after loop ileostomy

Xiaolong Li,*  Haitao Ma,* Yiming Sun,* Teming Li,* Cheng Wang,[†] Hong Zheng,[‡] Guoqing Chen,* Guangsheng Du,* Guangyan Ji,[§] Hua Yang,* Weidong Xiao* and Yuan Qiu*

*Department of General Surgery, Xinqiao Hospital, [†]College of Preventive Medicine, [‡]Department of Thoracic Surgery, Xinqiao Hospital, Army Military Medical University and [§]Department of Gastrointestinal Surgery, The First Affiliated Hospital of Chongqing Medical University, Chongqing, China

Key words

fecal diversion, intestinal barrier, intestinal homeostasis, loop ileostomy.

Accepted for publication 31 March 2022.

Correspondence

Dr Yuan Qiu or Dr Weidong Xiao, Department of General Surgery, Xinqiao Hospital, Army Military Medical University, Chongqing 400037, China. Email: xiaoq2037@qq.com and weidong.xiao@126.com

Xiaolong Li and Haitao Ma are co-first authors.

Declaration of conflict of interest: The authors declare that they have no potential financial conflict of interest related to this manuscript.

Author contribution: Yuan Qiu and Hua Yang contributed to the conception and design of the study. Xiaolong Li, Haitao Ma, Teming Li, and Cheng Wang analyzed and interpreted the patient data. Yiming Sun, Hong Zheng, Guoqing Chen, Guangsheng Du, and Guangyan Ji performed experiments and data collection. Xiaolong Li and Haitao Ma were a major contributor in writing the manuscript. Yuan Qiu and Weidong Xiao contributed to revising the manuscript. All authors read and approved the final manuscript.

Ethical approval: This research project was approved by the Medical Ethics Committee of Second Affiliated Hospital of Army Medical University, PLA (ethics number: 2020-YD056-01).

Abstract

Background and Aim: Intestinal homeostasis is closely associated with the normal intestinal luminal physiological environment. Temporary loop ileostomy changes the intestinal structure and diverts the fecal stream, thereby disturbing the intestinal environment. This study aimed to clarify the changing situation of the human intestinal mucosa barrier in the absence of a fecal stream after loop ileostomy.

Methods: We obtained paired samples from the fed (fecal stream maintained) and unfed (no fecal stream) portions of the loop ileostomy and subjected these samples to RNA sequencing. We also determined transepithelial electrical resistance. The mucus layer thickness and content of MUC2, tight junction proteins, and common antimicrobial peptides in ileum mucosa were studied.

Results: Transcriptome data revealed that genes associated with enhancing the intestinal barrier function of the unfed ileum were significantly decreased and genes associated with immune defense response were significantly increased. The transepithelial electrical resistance was lower and the mucus layer thickness was thinner in the unfed ileal mucosa than in the fed ileum. The MUC2, Occludin, and zonula occludens 1 content was lower in the unfed ileum than in the fed ileum. α -Defensin 5, α -defensin 6, and lysozyme content was higher in the unfed ileum than in the enterally fed ileum.

Conclusion: Intestinal barrier function is weakened after long-term fecal diversion, but antimicrobiota defense function is strengthened. Thus, the intestinal mucosa barrier adopts an alternative stable state during fecal diversion, which may explain the clinical paucity of cases of enterogenic infection caused by loop ileostomy.

Informed consent: Written consents were obtained from each patient.

Financial support: This research was funded by the Second Affiliated Hospital of Army Medical University "San Gao" and Nuclearized Military Medicine Innovation Project (grant number: 310921).

Introduction

Loop ileostomy is a common surgical procedure that is most commonly performed after low anterior resection for rectal carcinoma.¹ It may act as a safety mechanism to protect against sepsis in the event of a downstream intestinal anastomotic leak.² Fecal diversion can be achieved with an ileostomy, which forms an abdominal wall stoma to exude the proximal ileum contents.

After ileostomy, the enteric environment is interlinked with the outside world; the structure of the digestive tract is altered, which leads to no lumen content passing through the distal ileum but instead passing through the proximal ileum. These changes likely disrupt the primary homeostasis of the distal ileum. Studies have shown that fecal stream diversion mediated by loop ileostomy is associated with microbial dysbiosis,^{3,4} thereby driving a decrease

in obligate anaerobes and an increase in facultative anaerobes.⁵ Moreover, previous reports have also shown that the total mucosa thickness is reduced in the unfed ileum.⁶ An animal study in rabbits demonstrated that the loss of substances in the chyme after loop ileostomy may lead to Paneth cell hyperplasia.⁷

The maintenance of intestinal mucosal homeostasis depends on multimolecular and multicellular interactions in the gastrointestinal wall, which is destined to be a complex and delicate process.⁸ An impairment in this homeostasis may result in an enterogenic infection.⁹ However, in clinical practice, not many cases of enterogenic infection occur in these patients, despite drastic changes in the unfed ileum lumen environment, which suggests that a greater ecological tolerance may exist than previously recognized. We hypothesize that the intestinal mucosa barrier may adopt an alternative stable state during fecal diversion. However, to date, related research on this new intestinal state after loop ileostomy is insufficient. Therefore, this issue deserves further study.

The two ends of the ileum removed during ileostomy reversal surgery form a natural control specimen that is a beneficial tool for studying the barrier changes at both ends of the stoma. The aim of this study was to use such a specimen to clarify the changing situation of the barrier at both ends, based on a transcriptomic perspective, and to interpret interesting questions observed clinically with regard to intestinal homeostasis.

Materials and methods

Patients and methods. Ten patients with carcinoma of the rectum, who had undergone loop ileostomy and planned to undergo ileostomy closure, were recruited at the Second Affiliated Hospital of Army Medical University for this study. No patient had a history of other diseases besides rectal carcinoma. They were not using immunosuppressive drugs or antibiotics at the time of the investigation. The participants' demographics are in Table 1.

Loop ileostomy was performed on the oral side 30–50 cm from the terminal ileum in patients with rectal cancer. During the ileostomy closure, 10 cm of the oral and anal sides from the ileostomy were resected. The paired resected ileum segments were collected for this study (Fig. 1c). We defined “fed ileum” as the

tissue maintaining a fecal stream, and “unfed ileum” as the tissue with no fecal stream (Fig. 1a,c), as previously reported.¹⁰ The collected specimens were placed in ice-cold sterile normal saline (0.9%) and processed within 1 h of collection.

Histological examination and immunohistochemistry. The 4% paraformaldehyde fixed ileum tissue samples were embedded in paraffin and sectioned in 5- μ m thickness. The following primary antibodies were incubated overnight at 4°C: anti-mucin 2 (1:2000; Abcam, Cambridge, UK), anti-defensin 5 (1:50; Abcam), anti-defensin 6 (1:5000; Atlas, Bromma, Sweden), anti-LYZ (1:100; Abcam), anti-Occludin (1:100; Proteintech, Rosemont, IL, USA), anti-zonula occludens 1 (anti-ZO 1) (1:200; Abcam), and anti-Claudin 1 (1:700; Abcam). The sections were subsequently incubated for 60 min with a biotinylated secondary antibody (1:100; Zhongshan, Beijing, China). All histological images were captured under a light microscope (Leica, Wetzlar, Germany) at 200 \times magnification. Image-Pro Plus 6.0 (IPP6.0; Media Cybernetics, Inc., Rockville, MD, USA) was used for morphological analysis.

The inflammation score was determined by a blinded observer and was strictly based on a fully proven method that assigns a histological score of 0–4 to quantify the degree of inflammation. The criteria of this system include inflammatory cells, goblet cell depletion, immune infiltration, and architecture destruction.¹¹

Measurement of mucus thickness. The terminal 5 mm of the ileum was excised and immediately fixed in Carnoy's solution at 4°C for 4 h. It was then placed in 100% ethanol. The fixed ileum samples were embedded in paraffin, sectioned in 5- μ m thickness, and placed on glass slides. Tissue sections were stained with Alcian blue/periodic acid-Schiff (AB/PAS) stain. The average mucus layer thickness was obtained by taking 30 measurements within three fields at 200 \times magnification per section (six to eight sections per group).

Transmission electron microscopy. Transmission electron microscopy (TEM) samples were prepared using the same procedure, as previously described.¹² Cleaned ileal mucosal tissues were fixed with 4% glutaraldehyde. The tissues then underwent the standard treatments of fixation, dehydration, permeabilization, and embedding. The tissues were cut at 60-nm intervals and stained with uranyl acetate and lead citrate. The tissues were observed with TEM (JEM 1200EX; JEOL, Tokyo, Japan) and photographed with a digital camera.

Measurement of transepithelial electrical resistance. The ileum mucosa was quickly dissected from the muscular layer and mounted in an Ussing chamber (Physiologic Instruments, Inc., San Diego, CA, USA). This mucosal sample, which had an area of 0.5 cm², was then maintained on both sides of the Ussing chamber. The tissue was allowed to equilibrate in Krebs' solution, as described elsewhere.¹³ The transepithelial

Table 1 The participants' demographics

Age, mean \pm SD (years)	52 \pm 13
BMI, mean \pm SD	25.7 \pm 2.7
Sex, female/male	6/4
Days since ileostomy formation, mean \pm SD	192 \pm 48
Before ileostomy	
Obstruction symptoms, yes/no	0/10
TNM stage	
T2N0M0 I	3
T1N0M0 I	1
T3N0M0 IIA	2
T4aN0M0 IIB	2
T2N1aM0 IIIA	2

BMI, body mass index.

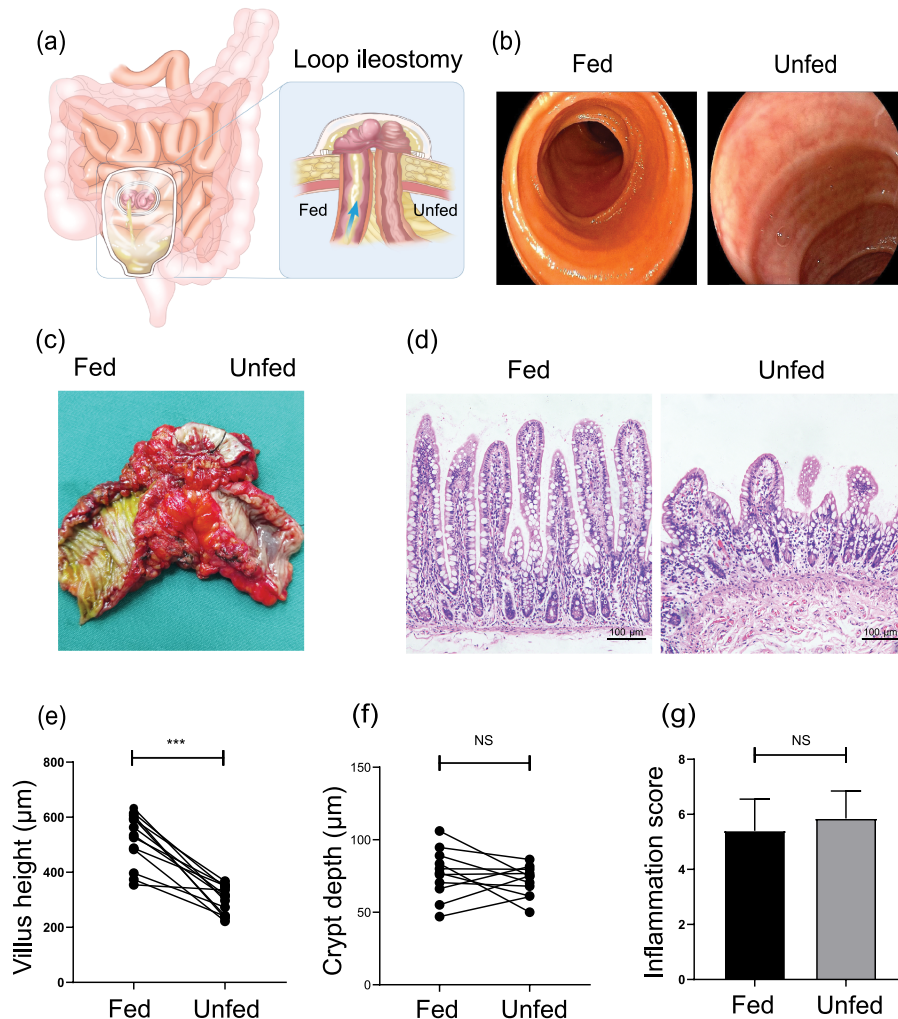


Figure 1 Fecal stream diversion mediated villus atrophy, but not inflamed. (a) The experimental model used in this study. The blue arrows denote the presence and direction of the fecal stream. (b) The endoscopic features of the fed and unfed ileum. (c) The mucosal features of the resected ileum. (d) Representative histological sections of the fed and unfed ileum stained with hematoxylin and eosin (H&E). Bars = 100 µm. (e, f) Villus height and crypt depth morphometric analyses of matched fed *versus* unfed ileum ($n = 10$). (g) The average histological inflammation score of the fed and unfed ileum ($n = 10$). Data were analyzed by using Student's *t* test. *** $P < 0.001$. NS, not significant.

electrical resistance (TER) was analyzed using the instrument-associated software Acquire & Analyze v2.3 (Physiologic Instruments, Inc.). The value of the TER is expressed as ohm-centimeter square ($\Omega \cdot \text{cm}^2$).

Intraepithelial lymphocytes preparation. Intraepithelial lymphocytes (IELs) were isolated, as previously described.¹⁴ In brief, the collected ileum was placed in Roswell Park Memorial Institute (RPMI) 1640 medium (Life Technologies, Frederick, MD, USA). The ileum mucosa tissue was washed in an IEL extraction buffer (5-mM ethylenediaminetetraacetic acid, 2-mM dithiothreitol, and 10% fetal bovine serum in phosphate-buffered saline) and cut into 5-mm pieces. The pieces were incubated in the extraction buffer and stirred continuously and rapidly for 30 min at 37°C. The tissue suspension was rapidly filtered through a glass wool column and centrifuged at 2000 rpm for 5 min at 4°C,

suspended in 20-mL 40% isotonic Percoll (Sigma-Aldrich, St. Louis, MO, USA), and centrifuged at 2200 rpm for 25 min at 4°C. The IELs constituted 40–70% of the interface. The cells were washed twice and resuspended in RPMI 1640 medium (Life Technologies).

Flow cytometric analysis. The IELs were stained with the following fluorescence-labeled monoclonal antibodies: cd3-bv421, cd8-percp5.5, and cd4-apc. All antibodies were obtained from BioLegend (San Diego, CA, USA). Cells were suspended in 80 µL of a staining solution (eBioscience, San Diego, CA, USA) with saturating the amounts of the antibodies and incubated for 30 min at 4°C in a dark environment. The apoptotic ratios for the IELs were measured using flow cytometry, based on the manufacturer's protocol. Flow cytometry was conducted using the standard techniques. Data acquisition and analysis were conducted using FlowJo software (Tree Star, Ashland, OR, USA).

RNA-Seq and data analysis. The total ribonucleic acid (RNA) for each sample was extracted using TRIzol (Invitrogen Life Technologies, Carlsbad, CA, USA), based on the manufacturer's instructions, and then delivered to Gene Denovo Biotechnology Co. (Guangzhou, China) for complete sequencing.

Statistical analysis. Data are expressed as the mean \pm standard error of the mean. Differences were analyzed using Student's *t* test with GraphPad Prism version 8.0 software (San Diego, CA, USA). Statistical significance was set at $P \leq 0.05$.

Results

Fecal diversion decreased villus height but not inflamed. Before closing the ileostomy, endoscopy was conducted to check for any obstruction in the downstream intestine. Endoscopic images showed that no fecal stream passed through the unfed ileum, the annular folds were apparently reduced (Fig. 1b,c), the mucosa was smooth, and the mucus covering the mucosal surface was significantly reduced. By contrast, the enterally fed ileum had a fecal stream and normal mucosal components (Fig. 1a,c).

After the continuity of the ileum was reconstructed, we collected resected ileostomy specimens (Fig. 1c). The analysis of mucosal morphometry revealed that the villus height was significantly reduced in the unfed ileum (Fig. 1d,e). However, no significant difference in crypt depth existed between the two groups (Fig. 1d,f). Compared with the enterally fed ileum, no significant difference was observed in the inflammation score (Fig. 1g).

Fecal stream deprivation was associated with the increased expression of immune process genes and the downregulation of intestinal barrier genes. An RNA sequencing genome-wide analysis was conducted on five paired fed and unfed ileum samples to identify biological processes and intestinal barrier-related genes affected by fecal

diversion. Among the 20 289 sequenced genes, we found 4513 genes that were differentially modulated by loop ileostomy and had a false discovery rate with a corrected P value < 0.05 (Fig. 2a). Among these, 1666 genes had a \log_2 -fold change > 1 or < -1 (Fig. 2a).

We next focused on genes related to the mechanical barrier of the intestinal mucosa. The heat map (Fig. 2b) shows that the genes *OCN*, *TJP1*, *TJP2*, and *TJP3*, which enhance intestinal barrier function,^{15,16} were decreased in the unfed ileum, whereas genes that increase intestinal permeability such as *CLDN2* and *CLDN10*^{17,18} were increased. Mucus barrier-related genes such as mucin 2 (*MUC2*) and mucin 3A (*MUC3A*) genes were significantly reduced in the unfed ileum (Fig. 2c).

In the unfed ileum, we conducted a gene ontology (GO) analysis of significantly upregulated genes and found that the immune response, defense response, response to molecules of bacterial origin, and antimicrobial humoral immune response mediated by antimicrobial peptides were overrepresented pathways (Fig. 3a). By contrast, intestinal absorption, nutrient metabolic processes, and hormone secretion were underrepresented pathways (Fig. 3a). The Kyoto Encyclopedia of Genes and Genomes (KEGG) analysis of the unfed ileum showed significantly upregulated genes involved in the Toll-like receptor signaling pathway, nucleotide-binding and oligomerization domain (NOD)-like receptor signaling pathway, and tumor necrosis factor (TNF) signaling pathway (Fig. 3b), whereas genes associated with protein, vitamin, and fat digestion; absorption; and metabolism were downregulated (Fig. 3b).

Fecal stream diversion decreases MUC2 expression and disrupts the intestinal mucus layer. Compared with the enterally fed ileum, the average thickness of the mucus layer in the unfed ileum was decreased, and the mucus layer was loosely adherent (Fig. 4a,b). MUC2 is the main secreted mucin that forms the mucus layer in the small intestine.¹⁹ Immunohistochemical staining showed that the expression of MUC2 was significantly reduced in the unfed ileum (Fig. 4c,d). We further photographed images under TEM. The aggregation number

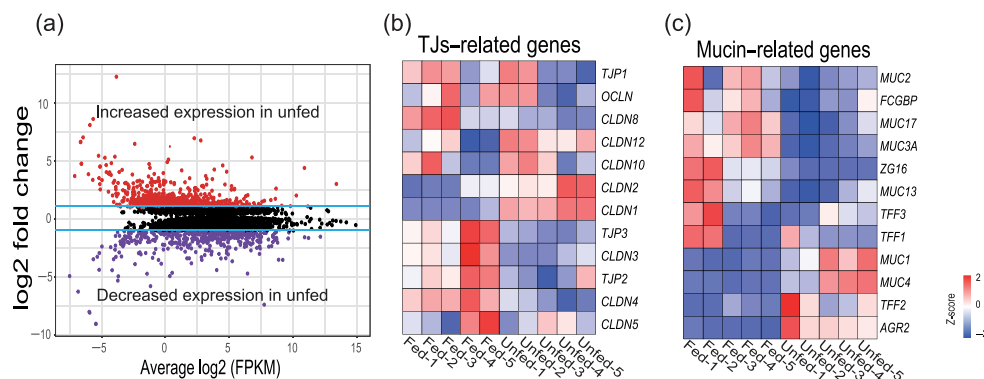


Figure 2 RNA sequencing shows significant changes between fed and unfed ileum. (a) The volcano plot shows differentially expressed genes between the fed and unfed ileum. A purple dot represents a gene with a false discovery rate (FDR) ≤ 0.05 and a \log_2 -fold change (\log_2 FC) < -1 . A red dot represents a gene with an FDR ≤ 0.05 and a \log_2 FC > 1 . Black dots indicate insignificant changes in gene expression. The blue lines indicate the cut-off values for a $1 - \log_2$ FC. (b,c) The heat map shows the differential expression of tight junctions (TJs) and mucin-related genes between the fed and unfed ileum. Each row represents one gene, and each column represents one sample. Red represents increased gene expression and blue-violet represents decreased expression.

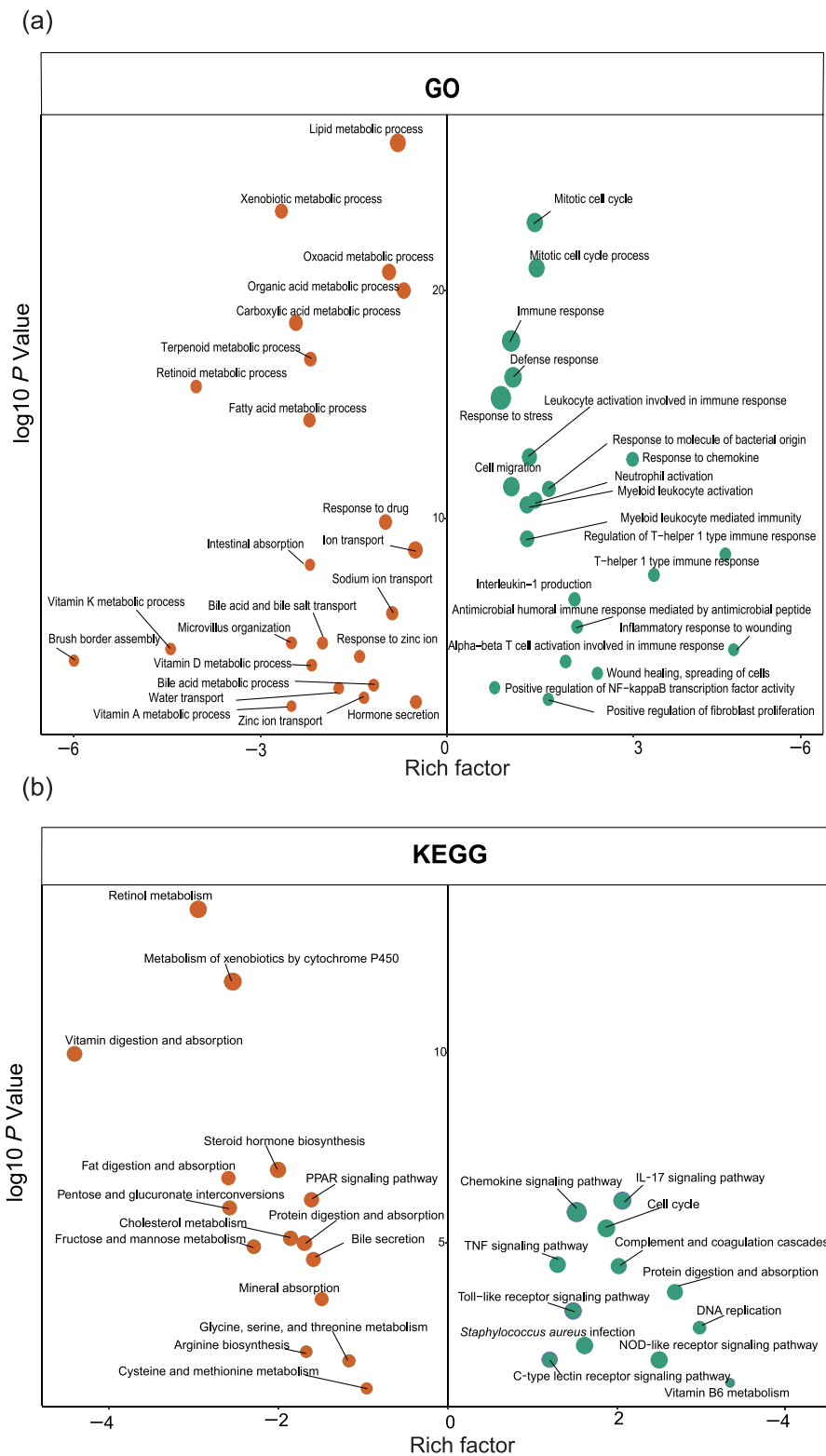


Figure 3 Differential regulatory status of biological processes in the unfed ileum. (a) The gene ontology (GO) analysis of upregulated and downregulated genes caused by fecal stream diversion. (b) The Kyoto Encyclopedia of Genes and Genomes (KEGG) analysis of upregulated and downregulated genes caused by fecal stream diversion. Circle size proportional represents the number of genes: (a) ●●●, 100; ●●●●, 200; ●●●●●, 300; and (b) ●●●, 10; ●●●●, 20; ●●●●●, 30. Green circles represent upregulated genes and orange circles represent downregulated genes with a false discovery rate corrected P value < 0.05 .

and the density of mucin granules in goblet cells of the unfed ileum were significantly less than those of the fed ileum (Fig. 4e,f).

Fecal stream deprivation impairs the mechanical barrier. The intestinal epithelial barrier of the fed and unfed ileum was assessed by measuring TER, using Ussing chambers. The results revealed that the unfed ileum had a significant lower TER than the enterally fed segments (Fig. 5a). In addition, the tissue content of Occludin, ZO-1, and Claudin-1 was determined by immunohistochemical staining. The expression of Occludin (Fig. 5c, d) and ZO-1 (Fig. 5e,f) was significantly decreased at the apex and base of the villus than in the unfed ileum. However, the analysis of the content of Claudin-1 (Fig. 5g,h) showed no significant difference between the two segments. The results of western blotting were consistent with the immunohistochemistry results (Fig. 5b).

Intraepithelial lymphocytes in the unfed ileum were reduced after fecal deprivation. Intraepithelial lymphocytes are one of the critical immunological compartments involved in the host immune defense system.²⁰ To detect changes in IELs in the unfed ileum, immunofluorescence staining and flow cytometry were conducted on 10 paired ileum samples. The data revealed that the number of CD3⁺ IELs in the unfed ileum was significantly reduced compared with that in the enterally fed limb (Fig. 6a,b). However, no significant difference existed in the proportion of CD4⁺/CD8⁺ IELs between the two groups (Fig. 6c,d).

Serum markers of infection were in the normal range during fecal stream diversion. We collected clinical data from the patients before ileum reversion surgery to determine whether the infection index of human serum would increase.

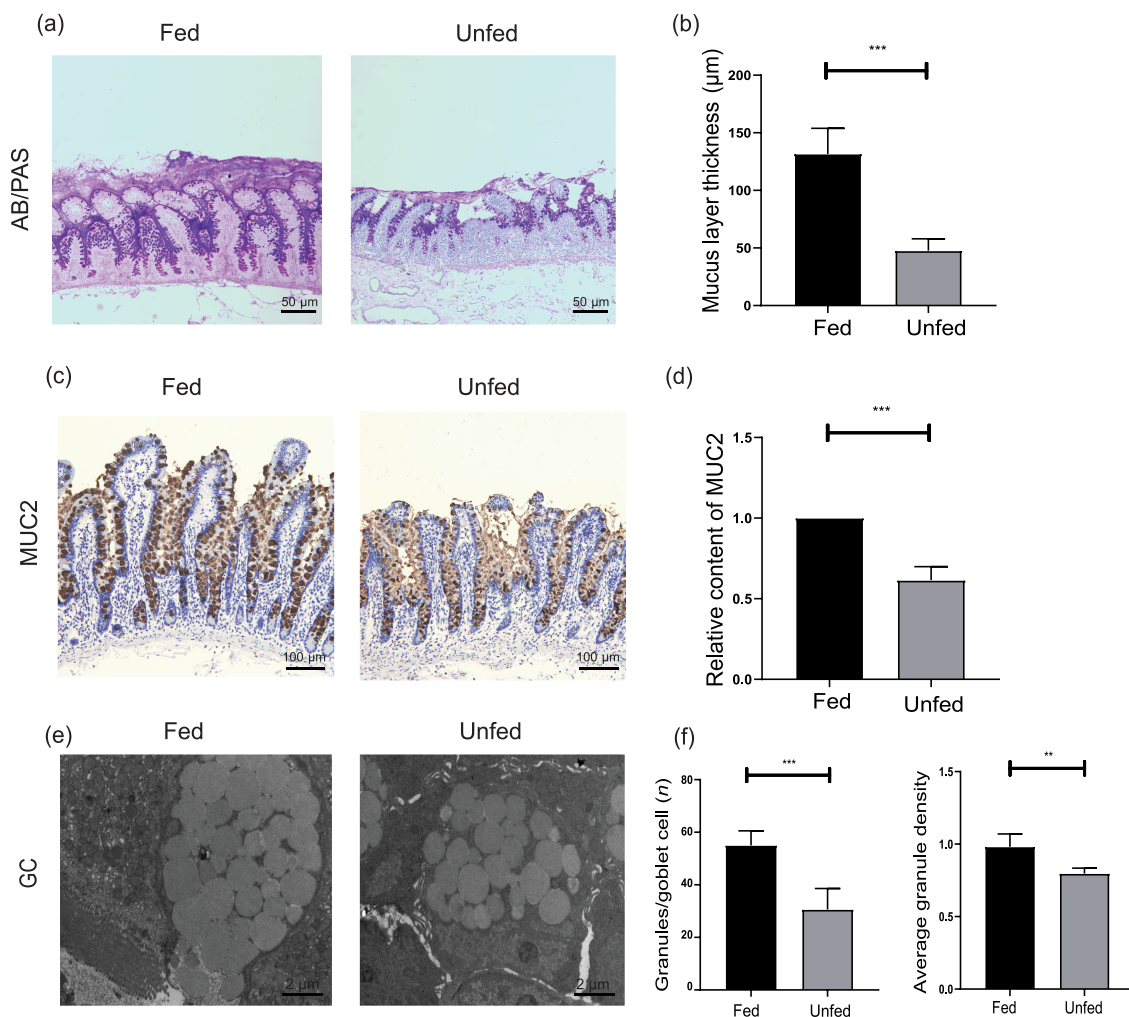


Figure 4 The mucus layer is impaired after fecal deprivation. (a) Representative histological sections of the fed and unfed ileum stained with Alcian blue/periodic acid-Schiff (AB-/PAS). Bars = 50 μm. (b) The histogram shows the statistical results of mucus layer thickness. (c) MUC2 immunohistochemical staining in the fed and unfed ileum. Bars = 100 μm. (d) The histogram shows the statistical results of immunohistochemistry. (e) Transmission electron microscopy (TEM) images of the fed and unfed ileum mucosa goblet cells. Bars = 2 μm. (f) The average granule density and the average number of mucin granules per goblet cell ($n = 10$ per group and 15 goblet cells evaluated per sample). Data were analyzed by using Student's *t* test. ** $P < 0.01$, *** $P < 0.001$.

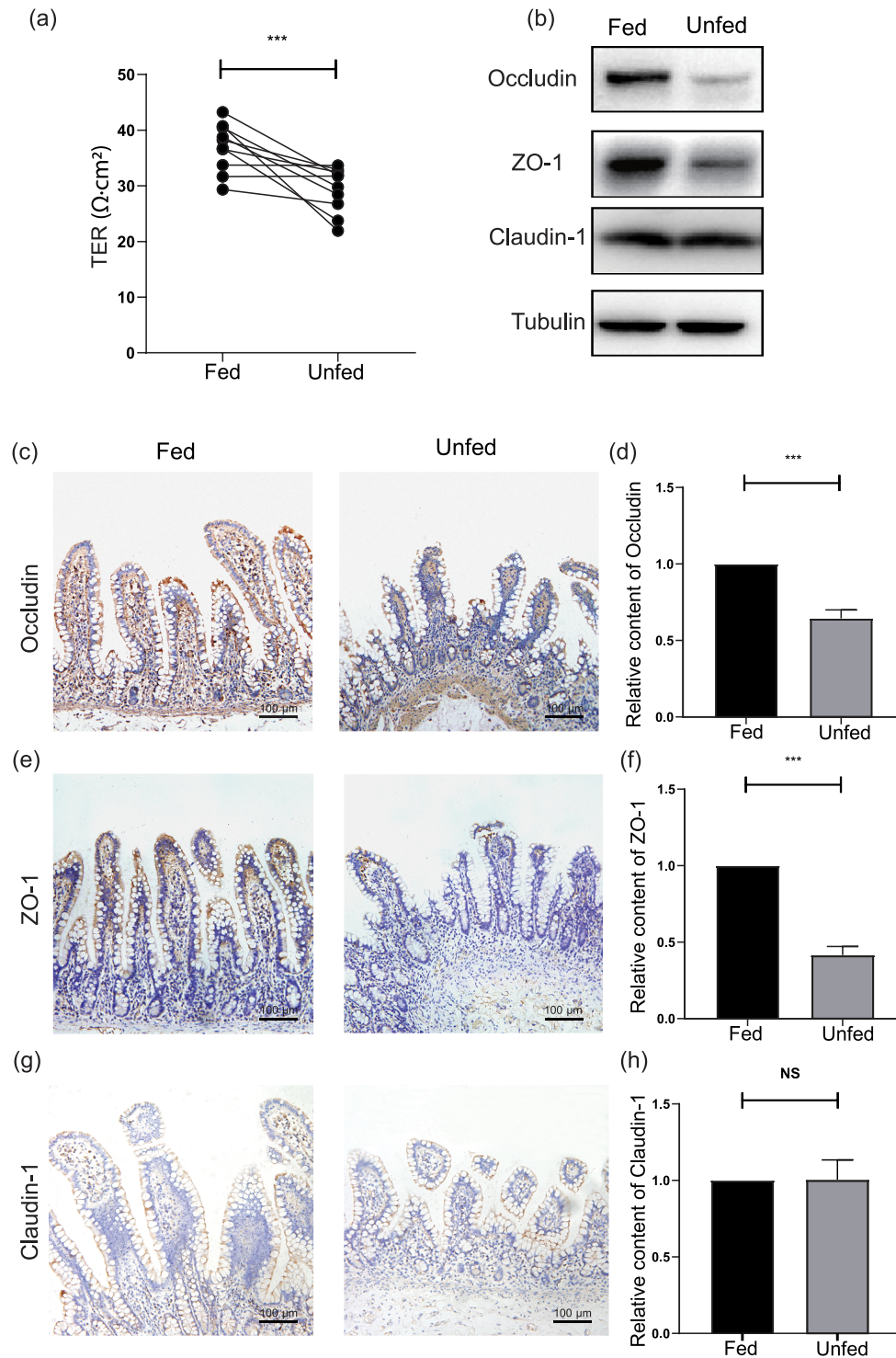


Figure 5 The mechanical barrier is disrupted after fecal stream diversion. (a) The transepithelial electrical resistance of the fed and unfed ileum. (b) The western blot analysis of the content of Occludin, Claudin-1, and zonula occludens 1 (ZO-1) between the fed and unfed ileum. (c) Occludin immunohistochemical staining findings in the fed and unfed ileum. Bars = 100 μm . (e) ZO-1 immunohistochemical staining findings in the fed and unfed ileum. Bars = 100 μm . (g) Claudin-1 immunohistochemical staining in the fed and unfed ileum. Bars = 100 μm . (d,f,h) The histogram presents the statistical results of the immunohistochemical findings. Data were analyzed by using Student's *t* test. ****P* < 0.001. NS, not significant.

Blood tests to measure the C-reactive protein level, neutrophil percentage, number of leukocytes, and the levels of interleukin-6, interleukin-8, and TNF- α are routinely used as predictors of clinical infection.²¹ Based on the data (Table 2), all serum marker indexes collected before closing the ileostomy were within the normal range.

Antimicrobial peptides were significantly increased in the unfed ileum. The aforementioned findings prompted us to further explore the changes in the intestinal mucosal immune effectors after fecal diversion. The transcriptomic analysis revealed that most genes associated with antimicrobial peptides were upregulated. The common antimicrobial protein genes *DEFA5*, *DEFA6*, *LYZ*, *REG3A*, *S1008A*, and *S1009A* were significantly increased in the unfed ileum (Fig. 7a). The findings of gene set enrichment analysis also suggested that the enrichment score of antimicrobial peptides was higher in the unfed ileum than in the enterally fed limb (Fig. 7b). In addition, based on immunohistochemical staining findings, the secretions of α -defensin 5 (HD5), α -defensin 6 (HD6), and lysozyme (LYZ) by Paneth cells at the base of the crypt were significantly increased in the unfed ileum compared with those in the enterally fed ileum (Fig. 7d–i). Western blot analysis revealed a similar result (Fig. 7c).

Table 2 Clinical data before ileum reconstruction

Clinical indicator	Results	Reference interval
CRP, mean \pm SD (mg/L)	4.8 \pm 1.6	0–8.0
WBC, mean \pm SD ($\times 10^9$)	5.1 \pm 1.2	4.00–10.00
Neutrophil percentage, mean \pm SD (%)	64.2 \pm 6.4	50.0–70.0
IL-6, mean \pm SD (pg/mL)	1.4 \pm 0.8	0–3.4
IL-8, mean \pm SD (pg/mL)	6.2 \pm 1.4	0–8.1
TNF- α , mean \pm SD (pg/mL)	24.4 \pm 18.3	< 62

CRP, C-reactive protein; IL-6, interleukin-6; IL-8, interleukin-8; TNF- α , tumor necrosis factor alpha; WBC, white blood cell.

Discussion

This study clarified the changing situation of the barrier at both ends of an ileostomy based on a transcriptomic perspective and investigated intestinal homeostasis. Our experiments demonstrated that fecal stream deprivation was associated with decreased villus height, a disrupted mucus barrier, and impaired function of the mechanical barrier of the unfed ileum mucosa. However, clinical data have a paucity of cases of enterogenic infection, despite the impairment of the unfed ileum mucosa barrier after loop ileostomy. In addition, transcriptome data showed that genes involved in immune responses and innate immune defense peptides were upregulated in the unfed limb. Furthermore, we demonstrated with

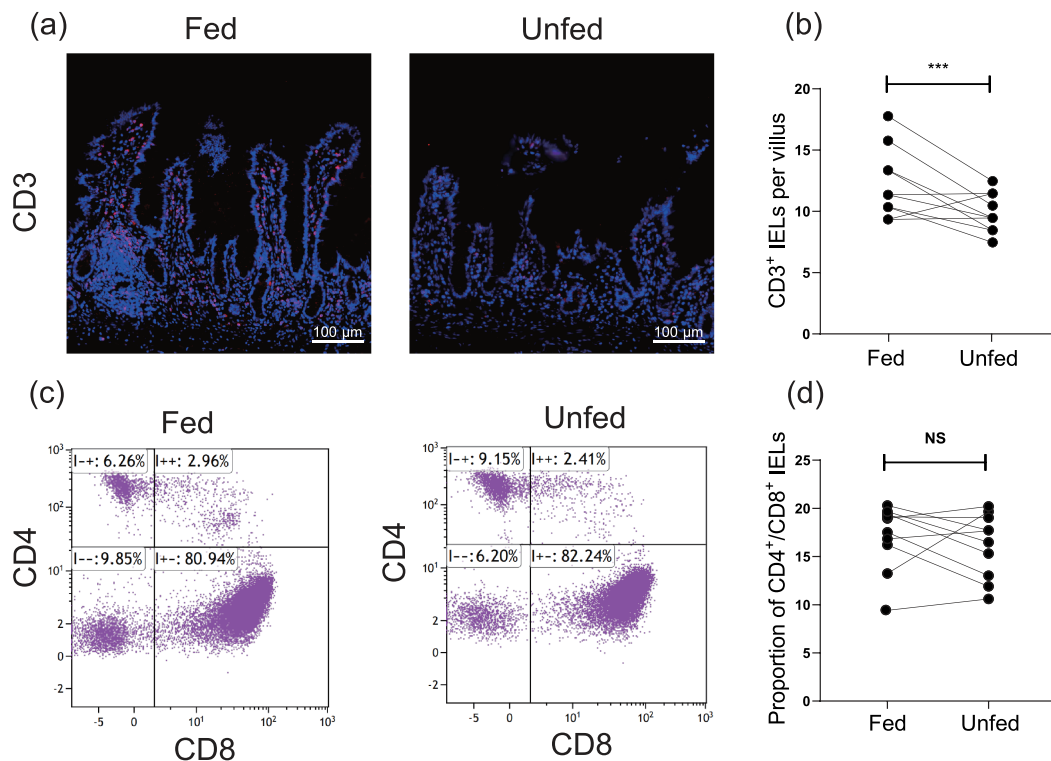


Figure 6 Differential status of intraepithelial lymphocytes (IELs) between the fed and unfed ileum. (a) CD3 immunofluorescence staining in the fed and unfed ileum. Bars = 100 μ m. (b) The counts of CD3⁺ IELs per villus in the fed and unfed ileum (n = 10). (c) Representative dot plots of CD4⁺ IELs and CD8⁺ IELs in the fed and unfed ileum. (d) The proportion of CD4⁺/CD8⁺ IELs in the fed and unfed ileum (n = 10). Data were analyzed using the Student's *t* test. ****P* < 0.001. NS, not significant.

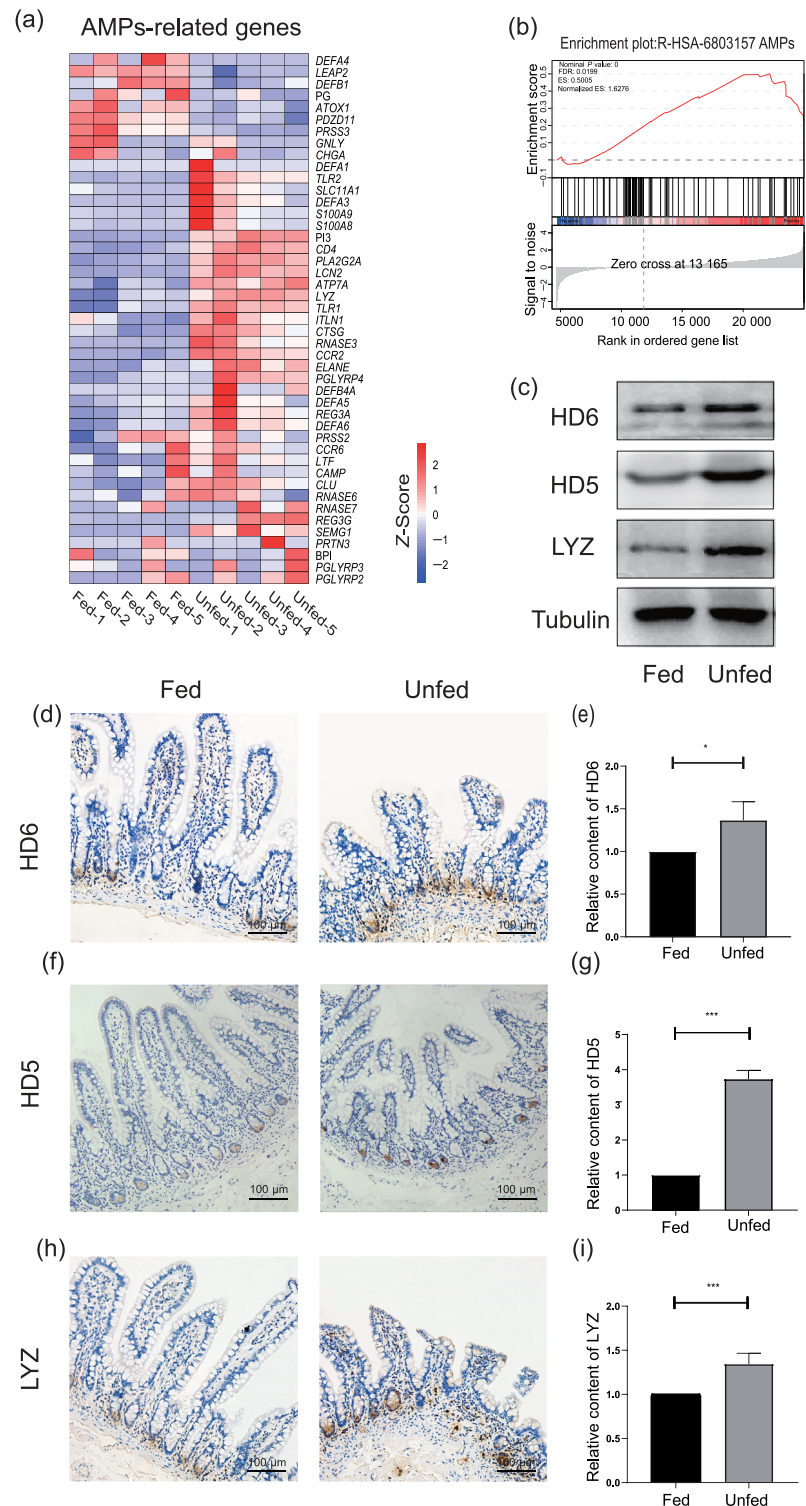


Figure 7 Fecal deprivation enhances the secretion of antimicrobial peptides. (a) The heat map shows the differential expression of antimicrobial peptides (AMPs)-related genes between the fed and unfed ileum. (b) Gene set enrichment analysis (GSEA) shows the enrichment score plot of antimicrobial peptides. (c) The western blot analysis of the content of α -defensin 6 (HD6), α -defensin 5 (HD5), and lysozyme (LYZ) between the fed and unfed ileum. (d) HD6 immunohistochemistry staining in the fed and unfed ileum. Bars = 100 μ m. (f) HD5 immunohistochemistry staining in the fed and unfed ileum. Bars = 100 μ m. (h) LYZ immunohistochemistry staining in the fed and unfed ileum. Bars = 100 μ m. (e,g,i) The histogram shows the statistical results of immunohistochemistry. Data were analyzed by using Student's *t* test. **P* < 0.05, ****P* < 0.001.

immunohistochemistry that innate immune antimicrobial peptides were increased in the unfed ileum, which suggested that immunological barrier function may be enhanced. These results provide novel insights into the effects of loop ileostomy on intestinal homeostasis.

Intestinal lumen chyme contains a large amount of nutrients, which have an important role in maintaining the growth and function of intestinal epithelial cells.²² The loss of chyme nutrients in the unfed ileum mucosa during fecal diversion may be associated with the destruction of the intestinal mechanical barrier and mucus

layer. MUC2 secreted by goblet cells is the main component of the mucus layer.²³ Recent studies have also shown that mechanical stimulation can promote goblet cells to secrete MUC2²⁴; loss of mechanical stimulation in unfed ileum caused by fecal stream diversion may be associated with the downregulation of goblet cell secretion.

The nutritional source of the intestinal microbiota differs from that of the intestinal epithelium, which can continue to receive nutrients from the blood after fecal diversion. By contrast, the intestinal microbiota derives its nutrition almost exclusively from chyme in the intestinal lumen. Investigators have reported that microbiota dysbiosis occurs at the phylum and genus levels in the unfed ileum after loop ileostomy.³ Another study has reported that the normal community in the ileum, which is dominated by strict anaerobes, becomes dominated by facultative anaerobes after loop ileostomy.⁵ These alterations may be partly explained by the introduction of oxygen via ileostomy into the normally anaerobic ileum.²⁵

Intraepithelial lymphocytes, generally considered the sentinels of the mucosal barrier, colonize the inter epithelium. Such colonization always depends on intestinal contents involved in some nutrients and the gut microbiome and its metabolites.²⁶ Our experimental data revealed that CD3⁺ IELs are downregulated in the unfed ileum, which was an adaption to the loss of intestinal contents. Previous studies have revealed that some intestinal contents such as short-chain fatty acids and indole derivatives of tryptophan can promote the differentiation and accumulation of IELs and maintain the balance of intestinal epithelium,^{27,28} which suggests that fecal deprivation in the unfed ileum may affect the abundance of IELs. Furthermore, the CD4⁺/CD8⁺ IEL ratio reflects the local immunity of intestinal mucosa.²⁹ In the physiological state, the CD4⁺/CD8⁺ IEL ratio is relatively constant. An abnormal CD4⁺/CD8⁺ IEL ratio in the intestinal mucosa can suggest inflammatory lesions in the gut.^{30,31} In relation to this finding, we found no difference in the proportion of CD4⁺/CD8⁺ IELs in the fed and unfed ileum. This finding suggested that the immune function of IELs remains relatively constant during fecal stream diversion.

Disturbances in the intestinal microbiota and impairment of the mucosal barrier are associated with enterogenic infection due to the induction of a proinflammatory state within the intestine.³² However, few cases clinically exist regarding enterogenic infection during fecal diversion in patients who undergo ileostomy. The clinical data we collected showed similar results with no significant increase in serologic-related indicators of infection. We speculate that this finding may be related to the reduced abundance or diminished virulence of intestinal microbiota. A balance between the gut microbiota and intestinal barrier may exist. If this balance is not disturbed, infections will not occur. It may also be related to some of the factors associated with enhancing natural immune biological processes that increase after fecal diversion.

Evidence has recently emerged indicating that antimicrobial peptides secreted by Paneth cells have vital roles in innate enteric immunity and in the regulation of intestinal microbiota.³³ In the human gut, α -defensin proteins, including α -defensin 5 and α -defensin 6, are the most abundant, diverse, and highly expressed antimicrobial proteins.³⁴ Previous studies have shown that α -defensin has spectral bactericidal activity against

gram-positive and gram-negative bacteria and, in some instances, against fungi, viruses, and protozoa.³⁵ However, few studies have focused on the exact impact of fecal stream deprivation on the secretion of antimicrobial peptides in the small intestine. In this study, our experimental data indicated that most antimicrobial peptide-related genes (i.e. *DEFA5*, *DEFA6*, *REG3A*, *LYZ*, *S1008A*, and *S1009A*) were upregulated and the secretion of common antimicrobial peptides (i.e. HD5, HD6, and LYZ) increased significantly in the unfed ileum after loop ileostomy. This finding may explain the clinical paucity of cases of infection, despite dramatic changes in the unfed ileum after loop ileostomy, which involves microbiota dysbiosis and impaired mucosal barrier.

Exploring the mechanism of increased antimicrobial peptide secretion caused by the loss of enteral nutrition is of great significance. RNA sequence data and GO analysis showed increased immune responses, defense responses, and neutrophil activation. The KEGG analysis showed that the Toll-like receptor signaling pathway, NOD-like receptor signaling pathway, TNF signaling pathway, and interleukin-17 signaling pathway were all enhanced. These signaling pathways have important roles in the secretion of antimicrobial peptides.^{36–38} Together with the aforementioned findings, we hypothesized that defective mucus and mechanical barriers may increase the chance of bacterial, fungi, viruses, and protozoa contact with epithelial cells, thereby altering microorganism-epithelial signaling and promoting an increase in immune and defense-related biological processes in the diverted unfed ileum.

In this study, we were only able to obtain ileal samples. In actuality, after the loop ileostomy, the colon was also in a foreign environment without a fecal stream. The colon is the primary reservoir for a large collection of commensal microbiota that produces many fermentation substances such as short-chain fatty acids, bile acids, and tryptophan. Intestinal commensal microbiota and their fermentation products are widely reported as having an essential role in maintaining intestinal homeostasis and integrity.^{39,40} In addition, they are involved in the maintenance of human health such as regulating blood pressure, promoting insulin secretion, and regulating blood sugar.^{41–43} However, what happens to the colon tissue and how the human body responds to these changes in the absence of a fecal stream needs further exploration.

In conclusion, we found that, although prolonged fecal diversion mediated by loop ileostomy disrupts the mechanical barrier and mucus layer of the intestinal mucosa, the secretion of natural immune antimicrobial peptides in the distal ileum is increased. This finding may explain the fact that, although loop ileostomy severely destroys the normal physiological environment of the distal ileum, few clinical cases of enterogenic infection exist. These results indicate that intestinal mucosal homeostasis is highly self-regulating and adequate to manage changes in the intestinal environment caused by loop ileostomy. Thus, a type of “dysbiotic equilibrium state” is achieved to maintain the stability of the intestinal environment during the period of fecal diversion.

Acknowledgments

None.

References

- Pellino G, Sciaudone G, Canonico S, Selvaggi F. Role of ileostomy in restorative proctocolectomy. *World J. Gastroenterol.* 2012; **18**: 1703–7. <https://doi.org/10.3748/wjg.v18.i15.1703>
- Lightner A, Pemberton J. The role of temporary fecal diversion. *Clin. Colon Rectal Surg.* 2017; **30**: 178–83. <https://doi.org/10.1055/s-0037-1598158>
- Beamish E, Johnson J, Shaw E, Scott N, Bhowmick A, Rigby R. Loop ileostomy-mediated fecal stream diversion is associated with microbial dysbiosis. *Gut Microbes* 2017; **8**: 467–78. <https://doi.org/10.1080/19490976.2017.1339003>
- Matsuzawa H, Munakata S, Kawai M *et al.* Analysis of ileostomy stool samples reveals dysbiosis in patients with high-output stomas. *Biosci. Microbiota Food Health* 2021; **40**: 135–43. <https://doi.org/10.12938/bmfh.2020-062>
- Hartman A, Lough D, Barupal D *et al.* Human gut microbiome adopts an alternative state following small bowel transplantation. *Proc. Natl. Acad. Sci. U. S. A.* 2009; **106**: 17187–92. <https://doi.org/10.1073/pnas.0904847106>
- Williams L, Armstrong M, Armstrong M, Finan P, Sagar P, Burke D. The effect of faecal diversion on human ileum. *Gut* 2007; **56**: 796–801. <https://doi.org/10.1136/gut.2006.102046>
- Keren D, Elliott H, Brown G, Yardley J. Atrophy of villi with hypertrophy and hyperplasia of Paneth cells in isolated (thiry-Vella) ileal loops in rabbits. Light-microscopic studies. *Gastroenterology* 1975; **68**: 83–93. [https://doi.org/10.1016/S0016-5085\(75\)80052-7](https://doi.org/10.1016/S0016-5085(75)80052-7)
- Franzosa E, Sirota-Madi A, Avila-Pacheco J *et al.* Gut microbiome structure and metabolic activity in inflammatory bowel disease. *Nat. Microbiol.* 2019; **4**: 293–305. <https://doi.org/10.1038/s41564-018-0306-4>
- Nagpal R, Yadav H. Bacterial translocation from the gut to the distant organs: an overview. *Ann. Nutr. Metab.* 2017; **71**: 11–6. <https://doi.org/10.1159/000479918>
- Wieck M, Schlieve C, Thornton M *et al.* Prolonged absence of mechanical stimulation in human intestine alters the transcriptome and intestinal stem cell niche. *Cell. Mol. Gastroenterol. Hepatol.* 2017; **3**: 367–88. <https://doi.org/10.1016/j.jcmgh.2016.12.008>
- Bramhall M, Rich K, Chakraborty A *et al.* Differential expression of soluble receptor for advanced glycation end-products in mice susceptible or resistant to chronic colitis. *Inflamm. Bowel Dis.* 2020; **26**: 360–8. <https://doi.org/10.1093/ibd/izz311>
- Patel K, Miyoshi H, Beatty W *et al.* Autophagy proteins control goblet cell function by potentiating reactive oxygen species production. *EMBO J.* 2013; **32**: 3130–44. <https://doi.org/10.1038/emboj.2013.233>
- Cheng J, Zhang L, Dai W *et al.* Ghrelin ameliorates intestinal barrier dysfunction in experimental colitis by inhibiting the activation of nuclear factor-kappa B. *Biochem. Biophys. Res. Commun.* 2015; **458**: 140–7. <https://doi.org/10.1016/j.bbrc.2015.01.083>
- Sun L, Li T, Tang H *et al.* Intestinal epithelial cells-derived hypoxia-inducible factor-1 α is essential for the homeostasis of intestinal intraepithelial lymphocytes. *Front. Immunol.* 2019; **10**: 806. <https://doi.org/10.3389/fimmu.2019.00806>
- Koliarakis I, Messaritakis I, Nikolouzakis T, Hamilos G, Souglakos J, Tsiaoussis J. Oral bacteria and intestinal dysbiosis in colorectal cancer. *Int. J. Mol. Sci.* 2019; **20**: 4146. <https://doi.org/10.3390/ijms20174146>
- Hunziker W, Kiener T, Xu J. Vertebrate animal models unravel physiological roles for zonula occludens tight junction adaptor proteins. *Ann. N. Y. Acad. Sci.* 2009; **1165**: 28–33. <https://doi.org/10.1111/j.1749-6632.2009.04033.x>
- Zeissig S, Bürgel N, Günzel D *et al.* Changes in expression and distribution of claudin 2, 5 and 8 lead to discontinuous tight junctions and barrier dysfunction in active Crohn's disease. *Gut* 2007; **56**: 61–72. <https://doi.org/10.1136/gut.2006.094375>
- Curry J, Tokuda S, McAnulty P, Yu A. Combinatorial expression of claudins in the proximal renal tubule and its functional consequences. *Am. J. Physiol. Renal Physiol.* 2020; **318**: F1138–46. <https://doi.org/10.1152/ajprenal.00057.2019>
- Ma S, Yeom J, Lim Y. Exogenous NAD stimulates MUC2 expression in LS 174T goblet cells via the PLC-delta/PTGES/PKC-delta/ERK/CREB signaling pathway. *Biomolecules* 2020; **10**: 580. <https://doi.org/10.3390/biom10040580>
- Konjar Š, Frising U, Ferreira C *et al.* Mitochondria maintain controlled activation state of epithelial-resident T lymphocytes. *Sci. Immunol.* 2018; **3**: eaan2543. <https://doi.org/10.1126/sciimmunol.aan2543>
- Calton E, Keane K, Newsholme P, Soares M. The impact of vitamin D levels on inflammatory status: a systematic review of immune cell studies. *PLoS ONE* 2015; **10**: e0141770. <https://doi.org/10.1371/journal.pone.0141770>
- Chen C, Wang Z, Li J *et al.* Dietary vitamin E affects small intestinal histomorphology, digestive enzyme activity, and the expression of nutrient transporters by inhibiting proliferation of intestinal epithelial cells within jejunum in weaned piglets. *J. Anim. Sci.* 2019; **97**: 1212–21. <https://doi.org/10.1093/jas/skz023>
- Cornick S, Kumar M, Moreau F, Gaisano H, Chadee K. VAMP8-mediated MUC2 mucin exocytosis from colonic goblet cells maintains innate intestinal homeostasis. *Nat. Commun.* 2019; **10**: 4306. <https://doi.org/10.1038/s41467-019-11811-8>
- Xu Y, Bai T, Xiong Y *et al.* Mechanical stimulation activates Piezo1 to promote mucin2 expression in goblet cells. *J. Gastroenterol. Hepatol.* 2021; **36**: 3127–39. <https://doi.org/10.1111/jgh.15596>
- Lauro A, Oltean M, Marino I. Chronic rejection after intestinal transplant: where are we in order to avert it? *Dig. Dis. Sci.* 2018; **63**: 551–62. <https://doi.org/10.1007/s10620-018-4909-7>
- Olivares-Villagómez D, Van Kaer L. Intestinal intraepithelial lymphocytes: sentinels of the mucosal barrier. *Trends Immunol.* 2018; **39**: 264–75. <https://doi.org/10.1016/j.it.2017.11.003>
- Cervantes-Barragan L, Chai J, Tianero M *et al.* *Lactobacillus reuteri* induces gut intraepithelial CD4CD8 α T cells. *Science (New York, NY)* 2017; **357**: 806–10. <https://doi.org/10.1126/science.aah5825>
- Ishizuka S, Tanaka S, Xu H, Hara H. Fermentable dietary fiber potentiates the localization of immune cells in the rat large intestinal crypts. *Exp. Biol. Med. (Maywood, NJ)* 2004; **229**: 876–84. <https://doi.org/10.1177/153537020422900903>
- Jaeger N, Gamini R, Cella M *et al.* Single-cell analyses of Crohn's disease tissues reveal intestinal intraepithelial T cells heterogeneity and altered subset distributions. *Nat. Commun.* 2021; **12**: 1921. <https://doi.org/10.1038/s41467-021-22164-6>
- Stallmach A, Schäfer F, Hoffmann S *et al.* Increased state of activation of CD4 positive T cells and elevated interferon gamma production in pouchitis. *Gut* 1998; **43**: 499–505. <https://doi.org/10.1136/gut.43.4.499>
- Hoytema van Konijnenburg D, Reis B, Pedicord V, Farache J, Victora G, Mucida D. Intestinal epithelial and intraepithelial T cell crosstalk mediates a dynamic response to infection. *Cell* 2017; **171**: 783–94. <https://doi.org/10.1016/j.cell.2017.08.046>
- Cani P, Possemiers S, Van de Wiele T *et al.* Changes in gut microbiota control inflammation in obese mice through a mechanism involving GLP-2-driven improvement of gut permeability. *Gut* 2009; **58**: 1091–103. <https://doi.org/10.1136/gut.2008.165886>
- Ji C, Deng Y, Yang A *et al.* Rhubarb enema improved colon mucosal barrier injury in 5/6 nephrectomy rats may associate with gut microbiota modification. *Front. Pharmacol.* 2020; **11**: 1092. <https://doi.org/10.3389/fphar.2020.01092>
- Alkaissi L, Winberg M, Heil S *et al.* Antagonism of adherent invasive *E. coli* LF82 with human α -defensin 5 in the follicle-associated epithelium of patients with ileal Crohn's disease. *Inflamm. Bowel Dis.* 2021; **27**: 1116–27. <https://doi.org/10.1093/ibd/izaa315>

- 35 Gallo R, Hooper L. Epithelial antimicrobial defence of the skin and intestine. *Nat. Rev. Immunol.* 2012; **12**: 503–16. <https://doi.org/10.1038/nri3228>
- 36 Asselin C, Gendron F. Shuttling of information between the mucosal and luminal environment drives intestinal homeostasis. *FEBS Lett.* 2014; **588**: 4148–57. <https://doi.org/10.1016/j.febslet.2014.02.049>
- 37 Gao X, Wan F, Mateo K *et al.* Bacterial effector binding to ribosomal protein s3 subverts NF- κ B function. *PLoS Pathog.* 2009; **5**: e1000708. <https://doi.org/10.1371/journal.ppat.1000708>
- 38 Thiébaud R, Esmiol S, Lecine P *et al.* Characterization and genetic analyses of new genes coding for NOD2 interacting proteins. *PLoS ONE* 2016; **11**: e0165420. <https://doi.org/10.1371/journal.pone.0165420>
- 39 Zelante T, Choera T, Beauvais A *et al.* *Aspergillus fumigatus* tryptophan metabolic route differently affects host immunity. *Cell Rep.* 2021; **34**: 108673. <https://doi.org/10.1016/j.celrep.2020.108673>
- 40 Sun R, Xu C, Feng B, Gao X, Liu Z. Critical roles of bile acids in regulating intestinal mucosal immune responses. *Therap. Adv. Gastroenterol.* 2021; **14**: 17562848211018098. <https://doi.org/10.1177/17562848211018098>
- 41 O'Connor K, Lucking E, Golubeva A *et al.* Manipulation of gut microbiota blunts the ventilatory response to hypercapnia in adult rats. *EBioMedicine* 2019; **44**: 618–38. <https://doi.org/10.1016/j.ebiom.2019.03.029>
- 42 Aarnoutse R, Ziemons J, Penders J, Rensen S, de Vos-Geelen J, Smidt M. The clinical link between human intestinal microbiota and systemic cancer therapy. *Int. J. Mol. Sci.* 2019; **20**: 4145. <https://doi.org/10.3390/ijms20174145>
- 43 Müller M, Hernández M, Goossens G *et al.* Circulating but not faecal short-chain fatty acids are related to insulin sensitivity, lipolysis and GLP-1 concentrations in humans. *Sci. Rep.* 2019; **9**: 12515. <https://doi.org/10.1038/s41598-019-48775-0>